

④ NA

⑤ 829800 7NA 8-1760

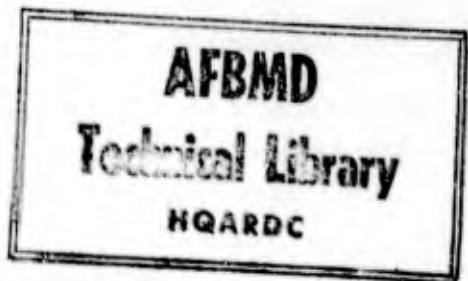
REG. NO. 18986

CONFIDENTIAL (P) U

eyl

LOG. NO. 22132

WDSOT _____



ITR-1409

OPERATION PLUMBBOB—PROJECT 1.8c

⑥

AIR-BLAST PHENOMENA AS AFFECTED BY TERRAIN, [U]

⑩

by L. M. Swift and D. C. Sachs.

Stanford Research Institute
Menlo Park, California

⑪

Issuance Date: December 6, 1957

⑫ 50 p.

⑬ NA

⑭ 4 1/2 NA

⑯ Proj. 1.8c
4-15-58

107-(1) m d

202-1-17 NA

FORMERLY RESTRICTED DATA

Handle as Restricted Data in foreign dissemination. Section 144b, Atomic Energy Act of 1954.

This material contains information affecting the national defense of the United States within the meaning of the espionage laws, Title 18, U.S.C., Secs. 793 and 794, the transmission or revelation of which in any manner to an unauthorized person is prohibited by law.

John W. Kodis
J. W. Kodis, Lt Col, USAF
Director, Program 1

⑰ AEC

⑱ ITR-1409

K. D. Coleman
K. D. Coleman, Col, USAF
Test Group Director, Programs 1-9

⑲ C

Ldc

CONFIDENTIAL

⑳ Report on
Operation Plumbob
[U]

ABSTRACT

The objective of Project 1.8c was to obtain data on ~~the~~ effects of gross variations of terrain upon a blast wave produced by a nuclear explosion, particularly at ground ranges of importance to moderately hard targets. On Shot Smoky (48 kt, 700-foot height of burst), total-head pressure, pitot-tube dynamic pressure, and overpressure were measured (1) on both sides of a ridge that rose 280 feet to a crest about 2,600 feet from ground zero and (2) at several equivalent ground ranges along relatively smooth terrain. ~~(for comparison with Item 1).~~

~~Results indicate that a~~ precursor formed over both ~~the~~ flat and ridge blast lines. The wave forms are not pure types and do not lend themselves to definite classification. Surface-level wave-front-propagation velocities indicate enhanced thermal effects on the front slope of the ridge and a strong diffraction effect as the wave passed over the top of the ridge.

~~Although there is evidence that surface level overpressure near the top of the ridge was depressed significantly,~~ generally, the ridge appeared to provide no real protection from overpressure, with increased overpressures noted on the front face and near the bottom of the back slope. However, the ridge appeared to offer considerable protection to drag-sensitive targets along the back slope and at the foot of the back slope.

No significant pressure spikes were observed on the ridge line; the precursor-type blast wave probably prohibited this effect. (C)

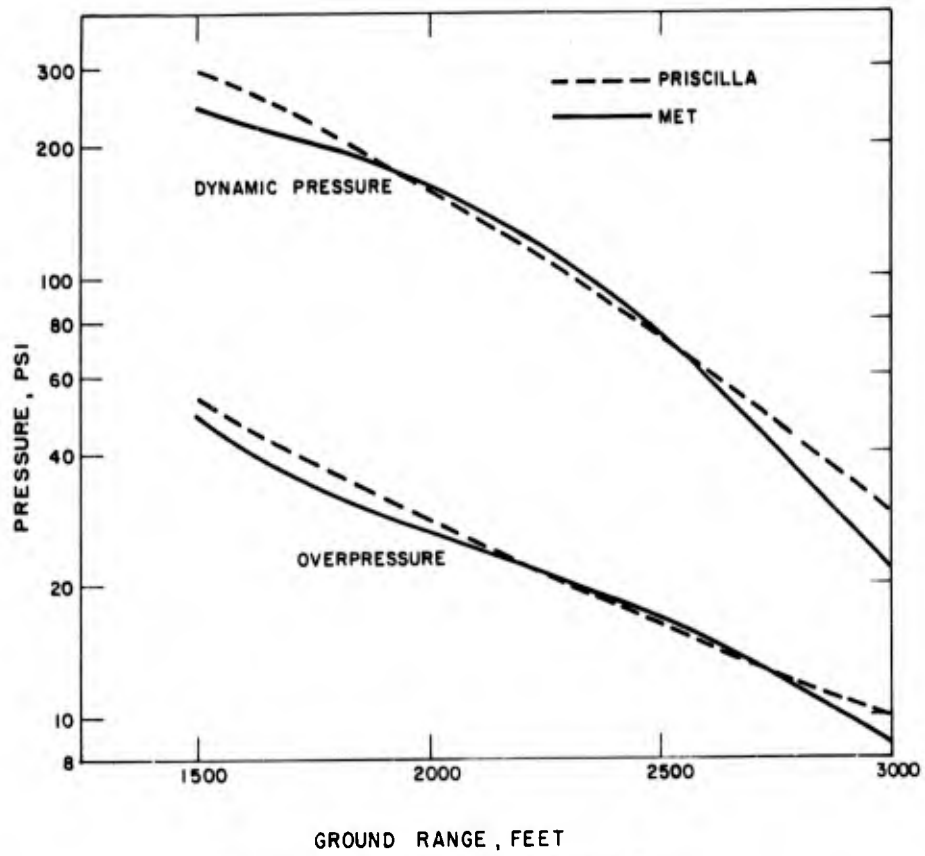


Figure 2.3 Met and Priscilla results, scaled to Smoky.

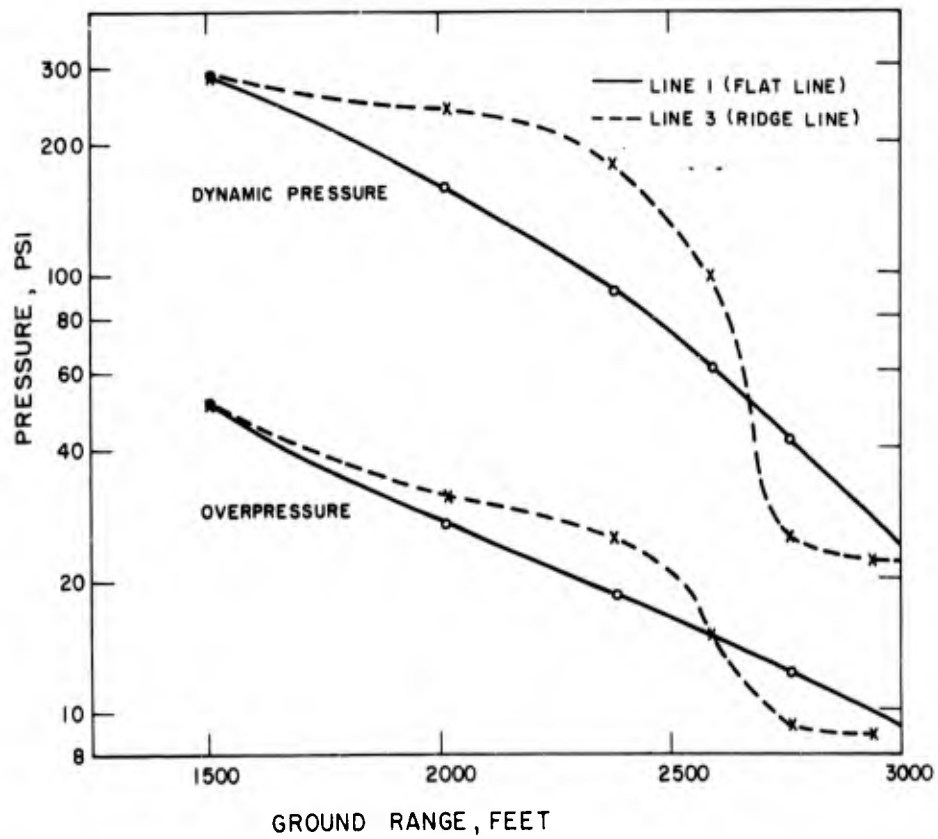


Figure 2.4 Smoky predictions.

The records of surface-level overpressure versus time, included in Figures 5.1 and 5.2, indicate that a well-established precursor wave progressed out from ground zero over Lines 1 and 3. The records have the characteristic hashy appearance of precursor pressure-time measurements. Figure 5.3 shows the results obtained from the static-overpressure

TABLE 5.1 OVERPRESSURE

Gage	Ground Range	Surface Elevation*	Gage Height	Arrival Time	Initial Precursor Pressure	Maximum Pressure	Time of Maximum	Wave Form Type †
11B	1,501	-58	0	0.314	25.5	32.0	0.508	1+
12B	2,018	-71	0	0.493	19.3	19.4	0.770	1+ or 2-
13B	2,381	-85	0	0.644	6.3	13.5	0.720	1+ or 2-
14B	2,589	-90	0	0.748	3.4	10.8	0.930	1+ or 2-
15B	2,760	-95	0	0.841	2.9	7.04	1.030	3
31B	1,501	+53	0	0.319	20.5	59.7	0.440	1
32B	2,018	+53	0	0.489	15.7	18.1	0.768	1+
33B	2,381	+195	0	0.623	12.4	17.5	0.838	3
34B	2,589	+280	0	0.721	—	2.65	0.765	3
34P3	2,589	—	3	0.721	—	11.3	0.757	2 or 3
34P10	2,589	—	10	0.727	—	10.4	0.762	2 or 3
35B	2,760	+220	0	0.874	—	6.65	1.102	4
35P3	2,760	—	3	0.874	—	9.50	0.927	3
35P10	2,760	—	10	0.876	—	9.77	0.930	3
36B	2,943	+170	0	1.005	—	12.2	1.071	3
36P3	2,943	—	3	1.006	—	12.8	1.075	3
36P10	2,943	—	10	1.008	—	11.4	1.070	3

* Referenced to ground zero approximate.

† For discussion and illustration of wave-form types see the appendix to this report and References 5 and 6.

gages mounted in the pitot-tube configuration 3 feet and 10 feet above ground on the top and back slope of the ridge. In general, the records of aboveground pressure versus time appear to be similar to corresponding surface-level records.

Figures 5.4 and 5.5 present the total-head and pitot-tube dynamic-pressure measurements from Lines 1 and 3, respectively. Generally, the records are similar to those

TABLE 5.2 DYNAMIC PRESSURE

Gage	Ground Range	Gage Height	Arrival Time	Maximum Total-Head Pressure	Maximum Dynamic Pressure	Time of Maximum
	feet	feet	sec	psi	psi	sec
12Z3	2,018	3	NR	NR	NR	NR
13Z3	2,381	3	0.651	44.5	33.4*	0.713
14Q3	2,589	3	0.791	—	28.5	0.824
14Q10	2,589	10	0.765	—	31.6	0.917
15Q3	2,760	3	0.879	—	21.1	0.943
15Q10	2,760	10	0.896	—	33.6	0.981
31Z3	1,501	3	0.319	277	250*	0.423
32Z3	2,018	3	NR	NR	NR	NR
33Z3	2,381	3	NR	NR	NR	NR
34Q3	2,589	3	0.743	—	21.4	0.914
34Q10	2,589	10	0.731	—	28.1	0.759
35Q3	2,760	3	0.875	—	5.28	0.935
35Q10	2,760	10	0.877	—	4.08	0.930
36Q3	2,943	3	1.006	—	4.25	1.078
36Q10	2,943	10	1.008	—	2.70	1.078

* These figures obtained by subtracting the instantaneous reading of surface-level overpressure from the maximum total-head pressure.

obtained during previous precursor-forming shots. It is believed that the excessive disturbance on the 31Z3 record (Figure 5.5) resulted from electrical disturbances, rather than actual pressure variations at the gage inlet.

Tables 5.1 and 5.2 present a summary of the Project 1.8c data. The tabulated data are as-read and must be considered as preliminary. Where dual channels were used to record identical measurements, an average of the two results is reported (except where one of the deflections was so small as to make its accuracy questionable).

Chapter 6

DISCUSSION

No effort is made in this report to derive any rigorous relationship between the phenomena observed and the geometry of the terrain or the pressure levels applied. The irregular, asymmetrical nature of the terrain and the limited number of measurement points prohibits any such attempt, particularly in an interim report. Rather, an attempt is made to observe the trends and general magnitudes of the effects and to compare them with the observed and derived effects of slopes on low-pressure shock waves.

6.1 WAVE-FORM CLASSIFICATION

Before attempting to discuss in detail the data obtained on Project 1.8c, the overpressure-time records will be examined on a purely qualitative basis. A detailed description of the SRI wave-form classification system is presented in Reference 5; however, the classifications are summarized in the appendix to this report. Table 5.1 presents the assigned classifications for the overpressure records obtained by this project.

Project 1.8c surface-overpressure wave-form types are plotted in Figure 6.1, a height-of-burst chart for overpressure wave forms. In general, aboveground wave forms are similar. The regions where the various types of wave form would be expected to appear (on precursor-forming shots) are labeled in the figure (Reference 5).

Initially, it should be stated that the pressure-time wave forms obtained on this project were generally not pure forms, i. e., most of the forms could not be placed unreservedly into a single classification. Nevertheless, looking at Figure 6.1 (and referring to the pressure-time records of Figures 5.1 through 5.3), it is evident that wave forms along the two blast lines were quite different.

It was expected that the first stations on each line would give about the same results; that this was apparently not so, hints at some asymmetry in the blast wave as it traveled out from burst point. Actually, the 31B record is a pure Type 1, whereas the control-line record (11B) shows significant deviations from the pure form.

At longer ground ranges, the wave forms indicate that the precursor dissipated more rapidly over the ridge line than over the flat line. These differences in wave form along the two lines are not severe, and due to the apparent asymmetry, it would be unwise to draw definite conclusions from such limited data.

No attempt will be made in this report to classify the wave forms associated with the dynamic-pressure measurements.

6.2 OVERPRESSURE

Peak values of observed overpressure are tabulated in Table 5.1 and are plotted against ground range in Figure 6.2. In the study of these data, reference should be made to the tracings of the pressure-time records of Figures 5.1 through 5.3, since they clarify some of the variations evident in the peak readings. In Figure 6.2, the solid line shows the variation of surface-level peak overpressure with ground range as measured on Line

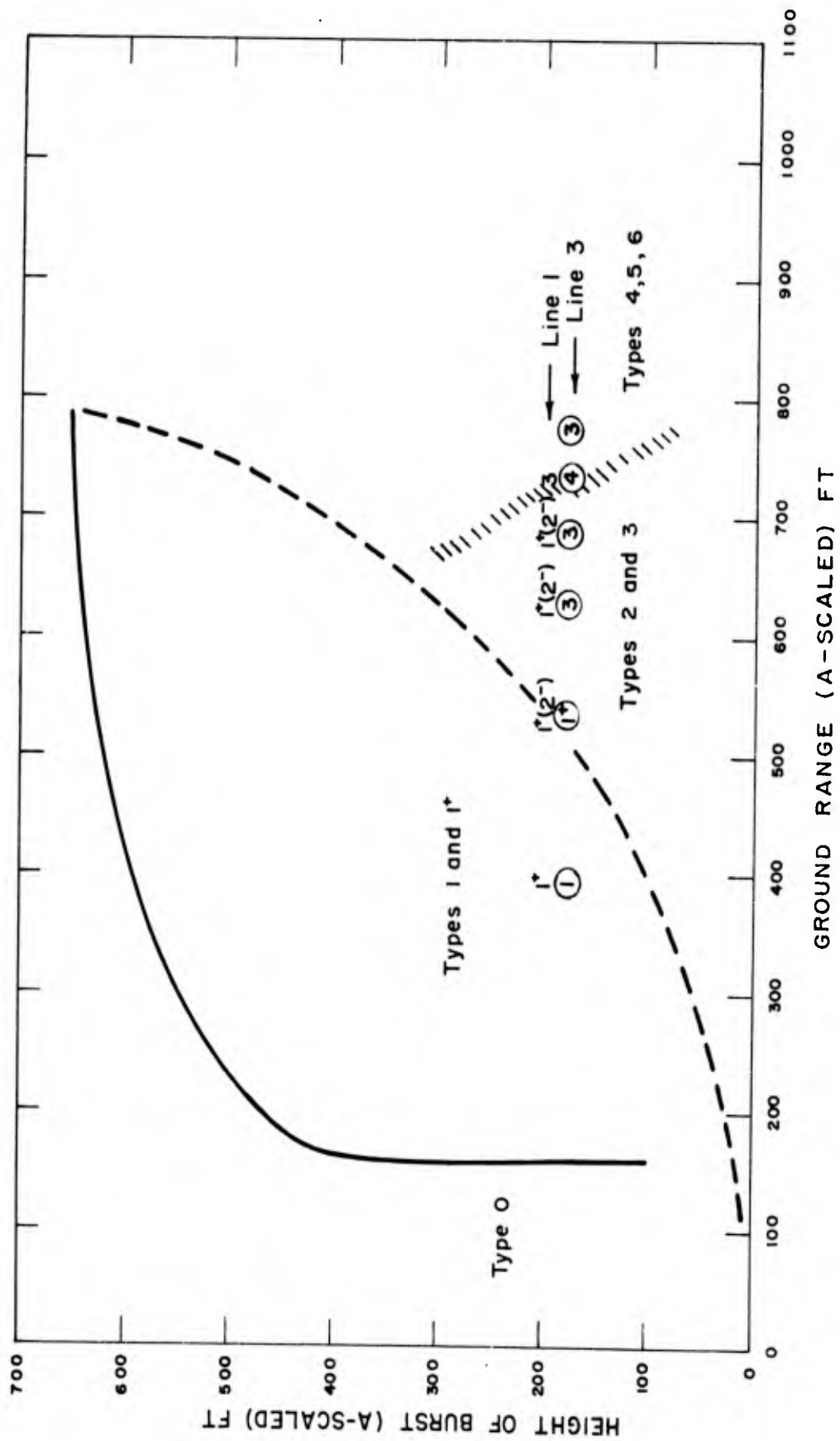


Figure 6.1 Height of burst for surface-level-overpressure wave forms.

1, the flat control line. The drop in pressure at 2,760 feet is unusual, but there is at present no reason to suspect the validity of this point. The regularity of this curve is in sharp contrast to that for Line 3, shown as a broken curve. Point-by-point examination of the data is necessary to interpret these variations.

At 1,501 feet, the Line 3 peak pressure was almost twice that of the flat line; although both stations were in flat terrain, the wave forms (11B and 31B, Figures 5.1 and 5.2) show a pronounced difference. Gage Record 31B is a typical Type 1 wave form, with the late peak value over twice that of the first pressure rise. Record 11B is somewhat atypical; it resembles a Type 2 form with the late peak, only slightly greater than the first peak, occurring somewhat later than that of 31B, although the 11B first arrival is slightly earlier. These features indicate that the precursor was more fully developed at this ground range on the flat line than on the ridge lines (see Section 6.1). At this state of precursor development, peak pressure is a very sensitive function of wave form.

At 2,018 feet, the peak pressures on the two lines were essentially equal, in spite of the fact that Station 32 on the ridge line was at the foot of the front slope. From previous experience with shock waves, a sharp spike might have been expected at the beginning of Record 32B. Its absence confirms the prediction of Section 1.3 that the slow rise of a precursor would prohibit this effect. If there was any increase in average pressure due to the slope, it has been masked in the record by other variations. (A difference may be evident when the curves are integrated to obtain total positive impulse.)

At 2,381 feet, the ridge-line peak overpressure was again higher than that of the flat line. The peak-pressure ratio is 1.3, very close to that predicted. It appears that here the rising slope did affect the overpressure meaningfully.

At 2,589 feet, the top of the ridge on Line 3, the peak value of Record 34B drops very markedly to about 25 percent of that of 14B, an effect which was not predicted but which might be expected in a sharply convex region where air-flow velocities are high.

The reduction of surface-level overpressure was greatly minimized, if present at all, at 2,760 feet on Line 3, a location near the middle of the back slope. At 2,943 feet, at the foot of the slope, there was again a pressure increase, even greater than the 30-percent increase at Station 33. Gage Record 36B at this station shows the only occurrence of what may be a spike. This, however, is small and cannot definitely be identified as a terrain effect.

Aboveground overpressures were measured at the last three stations on the ridge line and are shown in Figure 5.3, while the data are plotted in Figure 6.2. In contrast to the surface-level measurements, the data shows no reduction of the 3-foot peak pressure at the top of the ridge. There was no important difference in the 3-foot and 10-foot peak overpressures.

The terrain contours of Figure 2.1 show that the ridge line crossed the ridge near its end. There had been some concern as to the effects of diffraction around the end of the ridge upon the measurements at Stations 35 and 36. If such had been present to any extent, secondary peaks would be expected on the pressure-time wave forms from these stations. No such secondary peaks are evident.

From the standpoint of maximum overpressure, it is concluded that a ridge of the type studied offers no protection, except very near the surface in the sharply convex regions only. Overpressures are somewhat increased on the front face and near the bottom of the back slope.

6.3 DYNAMIC PRESSURE

Peak values of observed dynamic pressures are tabulated in Table 5.2 and plotted

against ground range in Figure 6.3. Again, in studying these data, reference should be made to the pressure-time records of Figures 5.4 and 5.5.

In Table 5.2, the fifth column lists the total-head pressure measured by these total-head gages that produced records. To reduce the data to approximate dynamic pressure, the corresponding record for surface-level overpressure was read at the time of maximum indicated in the seventh column. This value of overpressure was subtracted from the maximum total-head pressure to obtain the value of maximum dynamic pressure shown in the sixth column. Also in Table 5.2, arrival times shown are by no means as accurate as those for overpressure, due to the difficulty of determining the first departure of the slowly changing pressure-time record. No conclusions can be drawn from these arrival times as to the departures of the blast front from vertical, at least until more precise reading methods are applied.

Referring to Figure 6.3, the failure of Gage 12Z3 limited the data from the flat line to Stations 13, 14, and 15. Over this range, the values for 3-foot dynamic pressures (as read) show a reasonable decay with ground range; also, the 10-foot values are higher, which is in accord with previous experience. However, values for the two 10-foot peak dynamic pressures do not show a decay with increased ground range. There is no evident explanation for this minor anomaly.

The variation of 3- and 10-foot dynamic pressures on the ridge line is shown by the two dashed lines in Figure 6.3. The peak value of 250 psi at 1,501 feet is well documented and reasonable. Gage failures at the next two stations leave the shape of the curve between 1,501 feet and the top of the ridge in doubt. At the ridge top, the measured dynamic pressures were slightly lower than those on the flat line, but not significantly so. Both the wave forms and the ratio of dynamic pressure to overpressure show that precursor effects were still present at this range, to about the same extent on both lines. Also, on the ridge line the 10-foot-level dynamic pressure was higher than at 3 feet, as was the case on the flat line.

At the next station, on the back slope, the peak dynamic pressure dropped markedly below corresponding values on the flat line. The dynamic pressure ratio is about 0.25 at 3 feet, and about 0.12 at 10 feet. The 10-foot-level pressure was here lower than at 3 feet, a reversal of the usual circumstance. These conditions continued at the last station, at the foot of the back slope, where the maximum dynamic pressure continued to decrease, even though peak overpressure increased at this station. The measured values of dynamic pressure at this last station are about equal to the values predicted by Rankine-Hugoniot equations for a clean shock wave with a peak equal to the measured value of overpressure, even though the observed wave forms are not classic.

From the standpoint of dynamic pressure, it is concluded that a ridge of the type studied would offer a real protection to drag-sensitive targets on the back slope and at the foot of this slope. Lack of data prevents any conclusion as to effects on the front slope, but it seems reasonable to suppose that dynamic pressure should be enhanced, although this enhancement, if present, was not observed to hold over to the top of the ridge.

6.4 ARRIVAL TIME AND PROPAGATION VELOCITY

An examination of wave-front arrival times is frequently useful in analysis of precursor effects and other perturbations. Figure 6.4, a plot of the surface-level arrival times listed in Table 6.1, shows the time-distance curves for the two lines studied; the differences are obvious.

At the first station, at 1,501 feet, the earlier arrival was on the flat line, but by only about 5 msec. At 2,018 feet, the ridge-line arrival was earlier, and progressively more

so out to 2,589 feet, the top of the ridge. For about this point, there is a marked change in the slope of the curve, and the value for arrival at the next station is considerably later on the ridge line.

In Figure 6.5, these data are converted into terms of propagation velocity along the surface, corrected for slope (Table 6.1), and plotted against ground range. (The correction for slope does not change the general shape of the curve.) On the flat line, the velocity

TABLE 6.1 WAVE FRONT VELOCITY, SMOKY

Gage	Ground Range	Time of Arrival	Interval Velocity	Average Velocities	Terrain Slope	Velocity Correction for Slope
	feet	sec	fps	fps	degrees	fps
11B	1,501	0.314	2,890			
12B	2,018	0.493	2,405	2,648		
13B	2,381	0.644	2,000	2,203		
14B	2,589	0.748	1,840	1,920		
15B	2,760	0.941				
31B	1,501	0.319	3,045			3,045
32B	2,018	0.489	2,640	2,843	10	2,880
					12	2,700
33B	2,381	0.623	2,125	2,383	20	2,540
					16	2,210
34B	2,589	0.721	1,117	1,621	0	1,621
					-16	1,160
35B	2,760	0.874	1,396	1,257	-20	1,335
					-15	1,445
36B	2,943	1.005			-10	

decreased gradually with ground range, as is normal. On the ridge line, the first calculated value of velocity is higher than that for Line 1, although the earlier arrival time for the latter shows that at some closer ground range Line 1 velocities were higher. Although the ridge-line velocities did not actually increase on the front slope, they did not decrease as rapidly as those over the flat line, until near the top of the slope. As the ridge was passed, the Line 3 velocity dropped rapidly to approximately sonic velocity, then rose to join or exceed the velocity over the flat line.

The shape of the velocity curves appears to indicate enhanced thermal effects on the front slope (see Section 2.2.2), since the observed high velocity cannot be correlated with the small pressure increase observed on the front slope. The drop in velocity on the back slope was probably a combined effect of diffraction and of minimized thermal effects. Moreover, this low value is consistent with the observed dynamic pressures, since particle velocity must drop to permit a drop in propagation velocity.

6.5 FLAT-LINE COMPARISONS

Although the main objective of this project, namely to determine the effects of terrain variations upon blast waves, has been discussed in detail, it is germane to compare the flat-line data with results obtained previously in Nevada.

For peak surface-level overpressure the comparison is made in Figure 6.6. In this figure the TM 23-200 (Reference 7) curves for the average and poor surface conditions (scaled to Smoky yield and ambient pressure) are shown with the measured flat-line over-

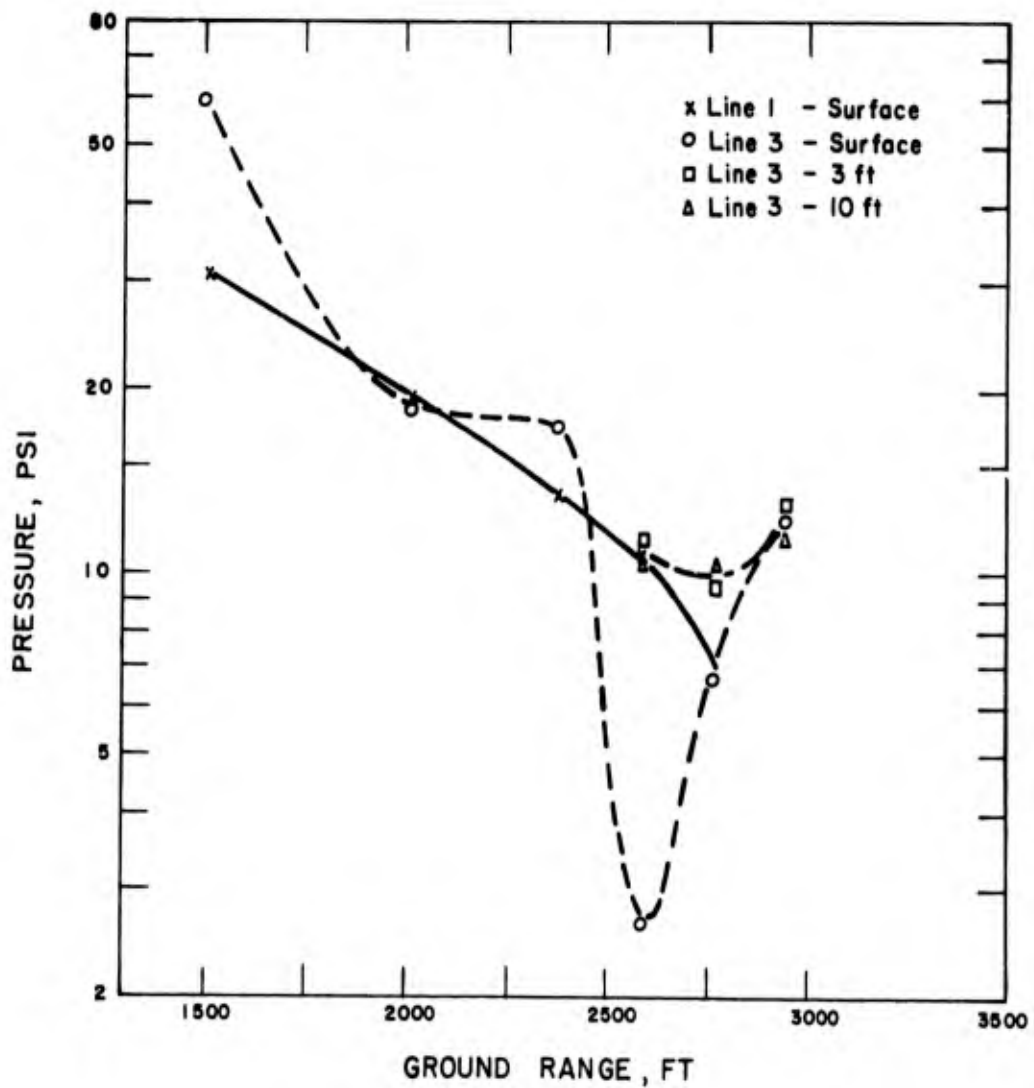
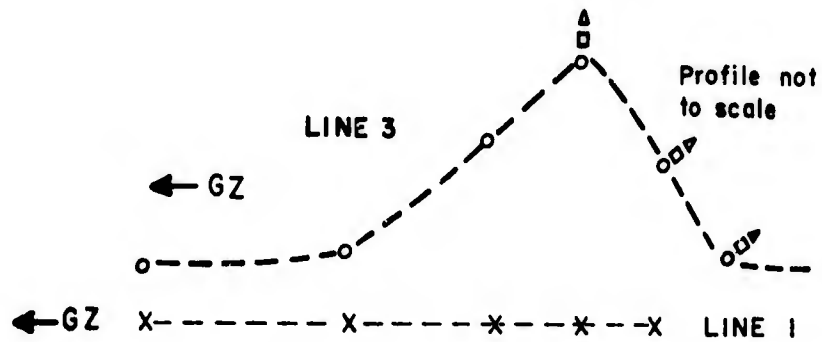


Figure 6.2 Peak overpressure versus ground range.

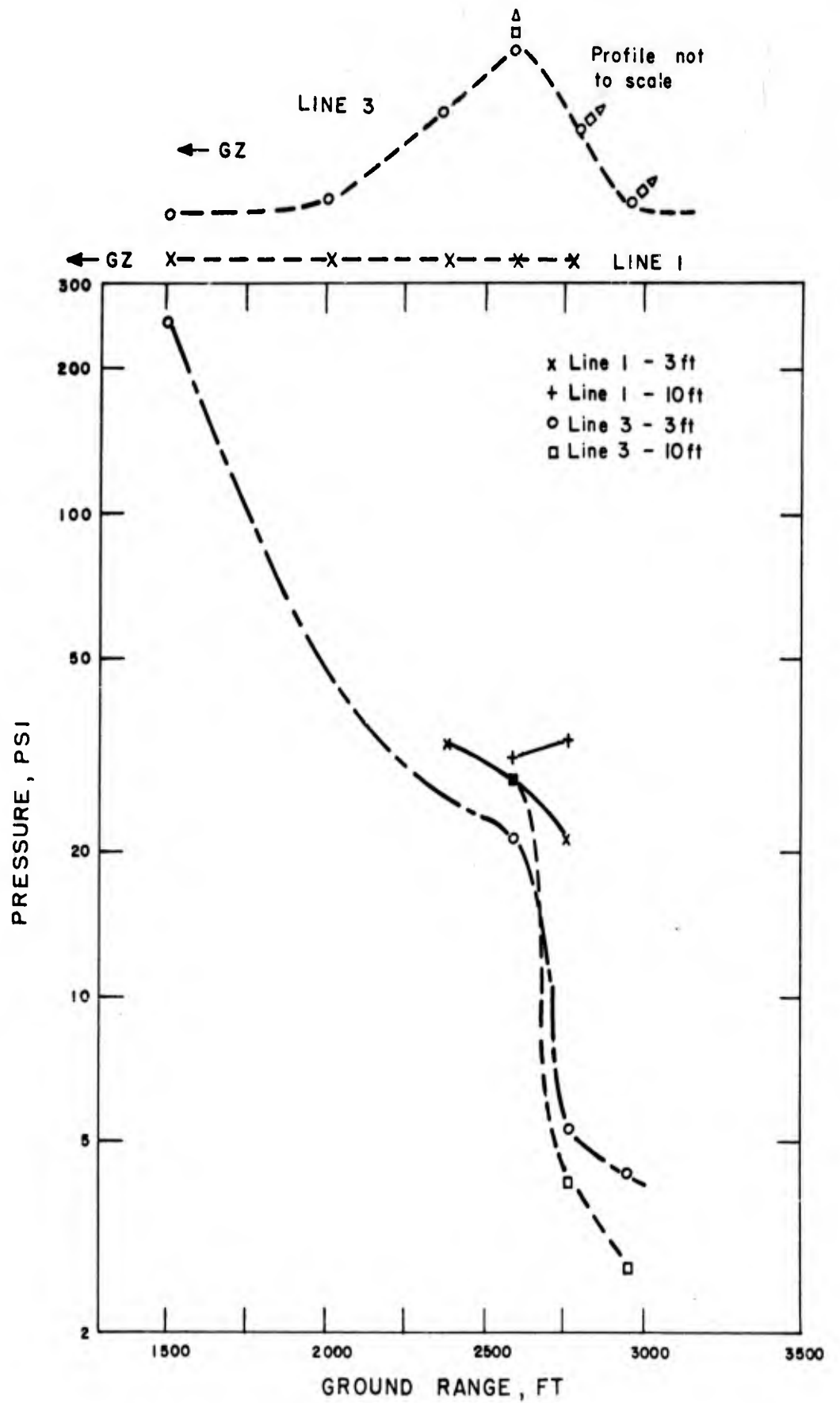


Figure 6.3 Peak dynamic pressure versus ground range.

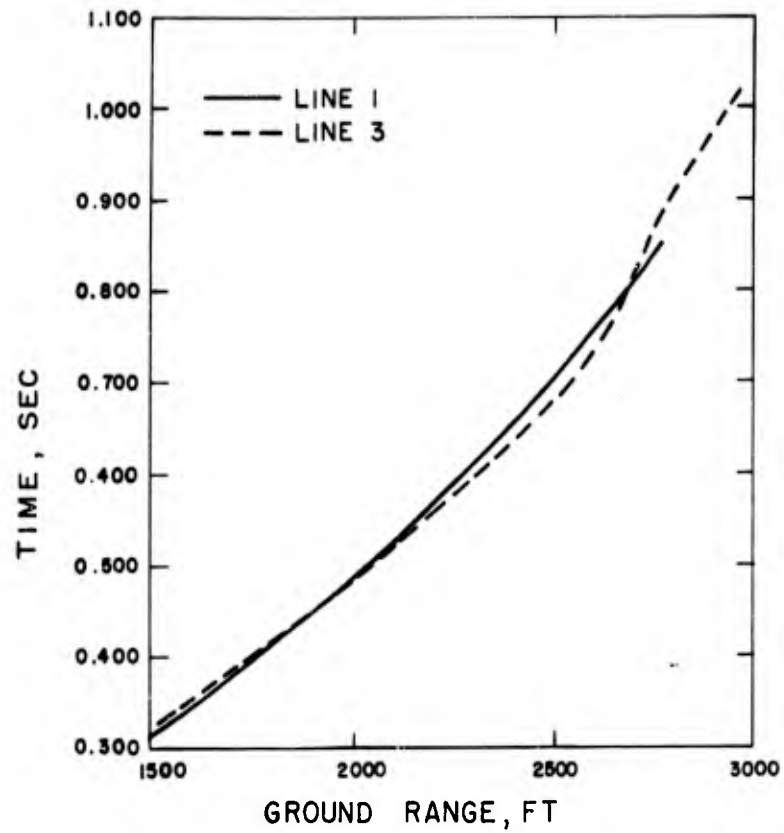


Figure 6.4 Arrival time versus ground range.

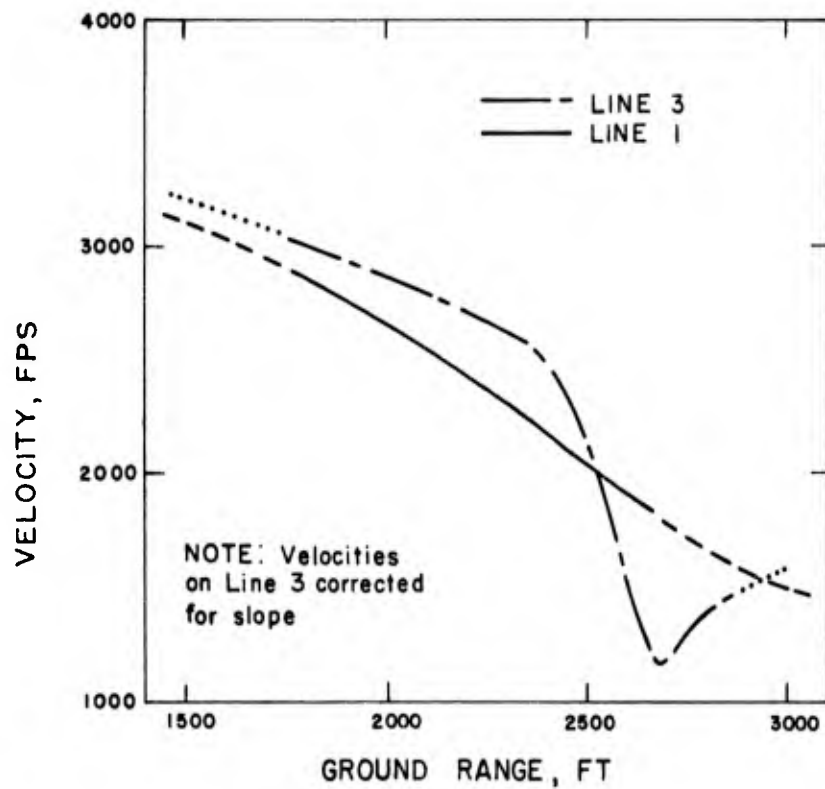


Figure 6.5 Propagation velocity versus ground range.

pressure curve. In general, the Smoky results agree best with the poor surface curve; however, it should be noted that the value for Station 31 on the ridge line is in better agreement with the average surface curve. This result may be due either to a geometrical asymmetry in the blast wave expansion or to a significant difference in surface characteristics along the two blast lines, or both.

Figure 6.7 shows the comparison between the Smoky flat-line dynamic-pressure data and an average curve obtained from the Priscilla and Met data. Where comparisons can be made, the data from previous shots show consistently higher peak dynamic pressures than observed on Smoky. Only at Station 31 on the ridge line (total-head gage) do the data

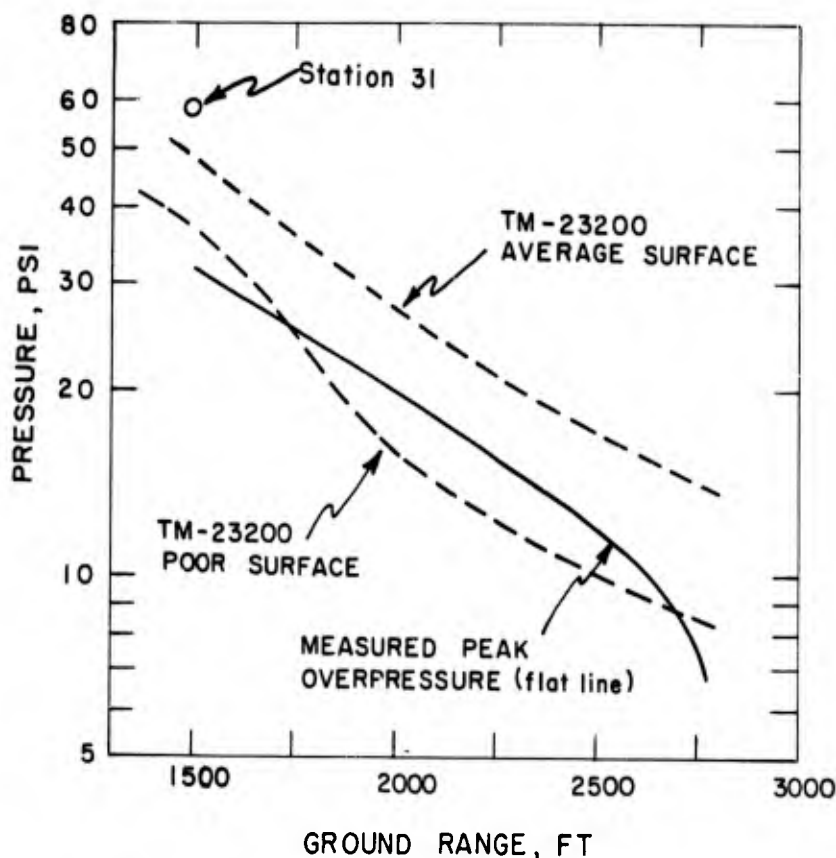


Figure 6.6 Measured peak overpressure compared with TM 23-200.

agree. The Priscilla and Met shots were detonated over a dust-covered Frenchman Flat area, whereas the Smoky area appeared to be more stabilized; an explanation for the discrepancy in measured dynamic pressure might involve these considerations. Further, if it can be assumed that measurements in regions of very-high dynamic pressure (above 100 psi) are not influenced appreciably by dust effects, then the agreement in data at the 1,500-foot range is more understandable.

6.6 INDICATIONS OF ASYMMETRY

It has been noted that the phenomena observed on the two blast lines differed in several respects that are not explained by the profile of the terrain. At the two front stations, the appearance of the overpressure wave forms, the value of the peak overpressure, and the time of arrival indicate that precursor effects were more advanced on Line 1 than on Line 3, even though this condition was reversed at later stations, pre-

sumably due to increased thermal effects on the front slope of Line 3. Two possible explanations for this observation have been advanced: (1) asymmetry of surface conditions in the vicinity of ground zero and (2) asymmetry of shielding introduced immediately underneath the nuclear device for diagnostic purposes.

A considerable area around the base of the tower was leveled and paved with asphalt for access and parking. The center of this area was southeast of the tower. In addition,

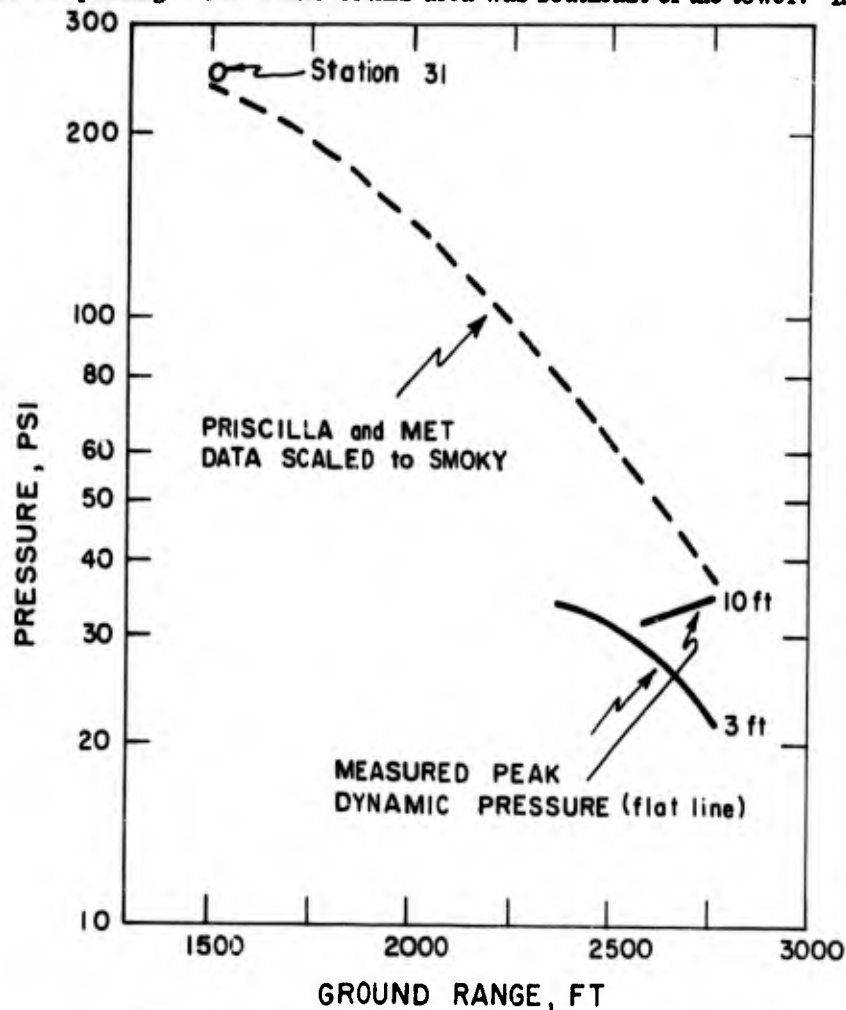


Figure 6.7 Measured peak dynamic pressure compared with Priscilla and Met data.

a paved road led from the tower along a line near Line 1, and several construction projects within 1,500 feet of ground zero in this direction removed the natural vegetation and increased the dustiness of the surface. These conditions may have been the cause of the observed asymmetry.

The shielding underneath the nuclear device has been reported as being centered along a line running north 30 degrees east and concentrated more heavily at the northerly end. From Figure 2.1, it appears that any thermal shielding caused by this local material would be more effective on Line 3 than on Line 1. It would also be more effective at very-short ground ranges. Such thermal shielding could cause the effects noted.

Further study and information on the local shielding are required to evaluate the relative importance of these two conditions and their probable contribution to the asymmetry observed. In any case, it does not seem likely that the general conclusions were importantly affected by this asymmetry or that the conditions described were responsible for the effects discussed in Section 6.5.

Chapter 7

CONCLUSIONS

There is evidence from pressure-versus-time wave forms, peak pressures, and times of arrival, that the Smoky blast wave, as observed at a radius of 1,500 feet, was asymmetrical. This may have been caused by surface conditions or by asymmetry of local shielding installed underneath the device, or both. This situation makes conclusions concerning the effects of the terrain less exact than was hoped, but probably does not affect the general conclusions.

Observations confirm that a precursor formed over both the flat and ridge blast lines; moreover, disturbed blast waves were evident at the farthest gage station on each line. Plots of the wave forms are not pure types and do not lend themselves to definite classification.

Since no significant peaking or pressure spikes are observed from results of the ridge-line overpressure measurements, it is concluded that the precursor-type blast wave prohibited this effect.

For overpressure, a peak-pressure ratio of about 1.3 was observed on the front slope of the ridge and at the foot of the back slope. Also, there is evidence that overpressures (near the surface only) at the ridge top were significantly depressed. Generally, the ridge studied offered no real protection from overpressure.




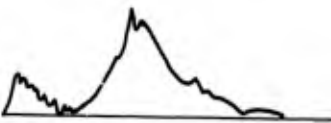


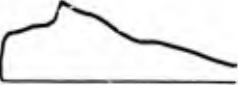
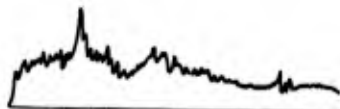
For dynamic pressure, it is concluded that a ridge of the type studied would offer significant protection to drag-sensitive targets along the back slope and at the foot of the back slope. Although it seems reasonable to suppose that the dynamic pressure would be increased on the front slope, lack of data prevents any definite conclusion on this effect.

Surface-level wave-front-propagation velocities indicate enhanced thermal effects on the front slope of the ridge and a strong diffraction effect as the wave passed over the top of the ridge.

Comparison of Smoky data with those of previous shots shows generally lower-than-predicted values of both peak overpressure and dynamic pressure. Increased thermal absorption and decreased dust loading due to surface conditions may explain these effects.

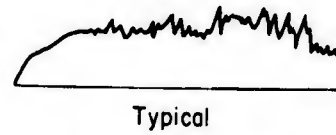
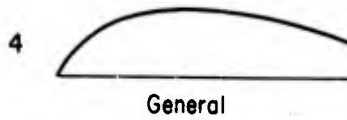
Appendix

OVERPRESSURE WAVE — FORM CLASSIFICATION

Type	Description of Form	Relation to Previous Type
0	<p>A sharp rise to a double-peaked maximum; peaks close together in time and approximately equal in amplitude.</p>	<p>In its ideal form, it is the classical single-peaked shock wave but is usually recorded as a double-peaked wave.</p>
	 <p>General</p>	 <p>Typical</p>
1	<p>A sharp rise to first low peak followed by either a plateau or a slight decay, then a higher second peak preceding the rapid decay. Time interval between first and second peaks can vary significantly; shock-like rises are evident.</p>	<p>The first low peak indicates the existence of a disturbance which travels faster than the main wave. This type is distinctly nonclassical.</p>
	 <p>General</p>	 <p>Typical</p>
2	<p>Same as Type 1 except that second peak is less than first.</p>	<p>The second peak has decayed to a lower value than the first and has become more rounded and less distinct. Second peak finally disappears.</p>
	 <p>General</p>	 <p>Typical</p>
3	<p>A first large, rounded maximum followed by decay; then a later, usually smaller, second peak. Pressure rises may be slower than for Type 2.</p>	<p>The first peak of Type 2 has developed to become the rounded maximum, while the second peak has decreased in magnitude with respect to the first.</p>
	 <p>General</p>	 <p>Typical</p>

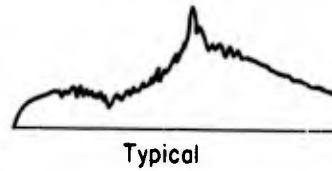
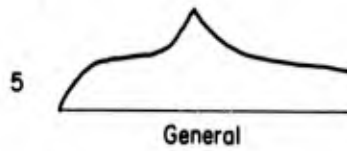
4 A long-rise-time flat-topped form which exhibits a long decay time and much hash.

The relatively sharp pressure rise of Type 3 has been replaced by a slow rise and the second peak has disappeared.



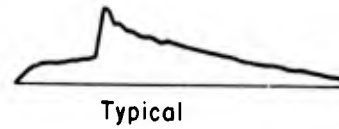
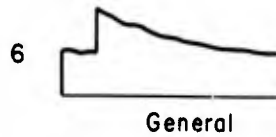
5 A pressure rise to a rounded plateau which is followed by a slow rise to a second, higher peak.

The single-peaked hashy form of Type 4 seems to develop a compression-type second peak, which may be the first indication of the return of the main wave.



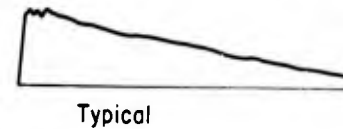
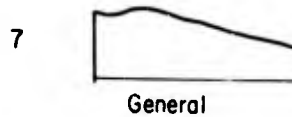
6 A clear-cut double peak form with a rise to a plateau which slopes upward, then a shock rise to a peak.

This is clearly a cleaned-up Type 5, with the compression-type second peaks becoming shocks.



7 A shock rise to a peak followed by either a slight gentle rise, a plateau, or in later examples, a slow decay.

The second peak of Type 6 has overtaken the first peak, resulting in a wave form which is close to classic; sharp, single peak is not evident.



7R Refers to Type 7 in region of regular reflection where a second (reflected) shock front is evident.

Second rise due to reflected wave.



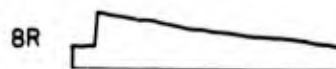
8 A classical wave form.

Sharp single-peaked form, followed by classic decay.



8R Refers to classical wave form in region of regular reflection.

Second rise due to reflected wave.



REFERENCES

1. Merritt, M. L.; "Air Shock Pressures as Affected by Hills and Dales"; Operation Tumbler-Snapper, WT-502; Sandia Corporation, Albuquerque, New Mexico; Confidential Restricted Data.
2. Merritt, M. L.; "Air Shock Pressures as Affected by Hills and Dales"; Operation Upshot-Knothole, WT-713; Sandia Corporation, Albuquerque, New Mexico; Secret Restricted Data.
3. Vaile, R. B., Jr., and Mills, L. D., LTJG, USN; "Evaluation of Earth Cover as Protection to Aboveground Structures"; Operation Teapot, WT-1128; Bureau of Yards and Docks, Washington, D. C.; Confidential Restricted Data.
4. Willoughby, A. B., Kaplan, K., and Condit, R. A.; "Effects of Topography on Shock Waves in Air"; Broadview Research and Development, WADC TR-56-289.
5. Sachs, D. C., Swift, L. M., and Sauer, F. M.; "Overpressure and Dynamic Pressure versus Time and Distance"; Operation Teapot, WT-1109; Stanford Research Institute, Menlo Park, California; Confidential Formerly Restricted Data.
6. Swift, L. M., Sachs, D. C., and Sauer, F. M.; "Air Blast Phenomena in the High Pressure Region"; ITR-1403; Stanford Research Institute, Menlo Park, California; Confidential Formerly Restricted Data.
7. Capabilities of Atomic Weapons, TM 23-200, July 1955; Department of the Army; Secret Restricted Data.